Available online at www.sciencedirect.com
SCIENCE DIRECT®
Thermochimica Acta 428 (2005) 77–81
thermochimica acta
www.elsevier.com/locate/tca

Mechanism and kinetics of thermal decomposition of 5-benzylsulfanyl-2-amino-1,3,4-thiadiazole

Xiao-Qing Shen[a,1], Zhong-Jun Li[b], Hong-Yun Zhang[b,*], Yi-Feng Zhou[b], Ke Liu[b], Qing-An Wu[b], Enbo Wang[a]

[a] *College of Chemistry, Northeast Normal University, Changchun 130024, China*
[b] *Department of Chemistry, Zhengzhou University, Zhengzhou 450052, China*

Received 12 August 2004; accepted 11 October 2004
Available online 21 November 2004

Abstract

A thiadiazole derivative, 5-benzylsulfanyl-2-amino-1,3,4-thiadiazole (BSATZ) was prepared. The single crystal structure of BSATZ was determined by X-ray diffraction and the thermal behavior of BSATZ in nitrogen was studied by TG and DSC. Based on the results of thermal analysis, the thermal decomposition mechanism of BSATZ in the temperature range of 100–400 °C was derived and the kinetic parameters have also been obtained. The decomposition of BSATZ in this temperature range acts as a model of two-step following reaction of $A \xrightarrow{F_n} B \xrightarrow{F_2} C$: an *n*th-order reaction (F_n) with $n = 2.16$, $E_1 = 111.59\,kJ\,mol^{-1}$, $\lg(A_1)\,(s^{-1}) = 8.82$ is followed by a second-order reaction (F_2) with $E_2 = 137.16\,kJ\,mol^{-1}$, $\lg(A_2)\,(s^{-1}) = 7.15$.

Keywords: 1,3,4-Thiadiazole; Crystal structure; Thermal decomposition; Kinetics

1. Introduction

Although the synthesis of 1,3,4-thiadiazole derivatives has been under study for many years, considerable attention continues to be given to these and related compounds since their properties can be greatly modified through the introduction of different substituents. Many of these compounds possess biochemical and pharmacological properties, especially their antimicrobial activity [1,2], which may afford them potential as therapeutic agents [3] and make them have a wide range of applications [4,5]. Synthesizing new 1,3,4-thiadiazole derivatives, determining their structures and investigating their thermal stability would therefore contribute to developing new medicament and provide basic data for the further pharmacology research.

Because of their antidepressant and anxiolytic activity, substituted 5-thiol-2-amino-1,3,4-thiadiazoles such as 5-benzylsulfanyl-2-amino-1,3,4-thiadiazole (BSATZ), which is formed by the covalent combination of 5-thiol-2-amino-1,3,4-thiadiazole moiety with benzyl group through the sulphur atom, have been studied both in the fields of synthesis and characterization by spectroscopic analysis [6,7]. However, the single crystal structures and the thermal behaviors of these compounds are rare to literature. Up until now no detailed investigation has been under taken into the single crystal structure, the thermal behavior and decomposition kinetics of the compound BSATZ. In the present paper, we report the single crystal structure and thermal behavior of BSATZ. The kinetic parameters of decomposition of this compound have been calculated by employing model-free method and the reaction model has been derived by means of non-linear regression.

* Corresponding author. Tel.: +86 3717763675; fax: +86 3717761744.
E-mail addresses: shenxiaoqing@zzu.edu.cn (X.-Q. Shen), wzhy917@zzu.edu.cn (H.-Y. Zhang).
[1] Present address: College of Material Engineering, Zhengzhou University, Zhengzhou 450052, China.

0040-6031/$ – see front matter © 2004 Published by Elsevier B.V.
doi:10.1016/j.tca.2004.10.002

2. Experimental

2.1. Materials

BSATZ used in this research work was prepared according to the following method: to a mixture of 5-thiol-2-amino-1,3,4-thiadiazole [8] (2 g, 15.04 mmol) and Na_2CO_3 (2.4 g, 28.9 mmol) in DMF (40 ml), benzyl chloride (2 ml) was added dropwise and the mixture was stirred and refluxed at about 100 °C for 6 h. By cooling overnight, the precipitates were obtained by being filtrated and recrystallized in EtOH. Yield 68%. Found: C, 48.52; H, 4.05; N, 18.36%. Anal. Calc. for $C_9H_9N_3S_2$: C, 48.40; H, 4.06; N, 18.82%. In order to get single crystal, pure products were dissolved with stirring for 30 min. After few days, bright yellow crystals suitable for X-ray measurement were obtained. Dimensions of a single crystal were 0.15 mm × 0.15 mm × 0.20 mm.

2.2. Experimental equipment and conditions

In the determination of the structure of the single crystal, X-ray intensities were recorded by a Rigaku-Raxis-IVX-ray diffractometer using graphite-monochromated Mo Kα radiation (λ = 0.71073 Å) at 293(2) K, 3038 reflections were measured over the ranges $1.76 \le 2\theta \le 27.46$, $-32 \le h \le 7$, $-7 \le k \le 7$, $-16 \le l \le 18$, yielding 1886 unique reflections. Raw data were corrected and the structure was solved using the SHELX-97 program. Non-hydrogen atoms were located by direct phase determination and subjected to anisotropic refinement [9]. The full-matrix least squares calculations on F^2 were applied on the final refinement. The refinement converged at $R_1 = 0.0586$ and $wR_2 = 0.1265$ values for reflections with $I > 2\sigma(I)$. Details of crystal structure determination are described bellow. Full atomic data are available as a file in CIF format.

The thermal decomposition experiments were carried out using NETZSCH TG 209 and DSC 204 instruments in nitrogen atmosphere with a flow rate of 20 and 70 ml min^{-1}, respectively. In these experiments the crystals were pretriturated. An Al crucible was used for DSC measurement and Al_2O_3 crucibles for TG to hold about 3–5 mg of the samples. The heating rate for thermal decomposition employed was 10 °C min^{-1}, and the rates for kinetic analysis were 4.8, 14.7, 19.7 and 29.90 °C min^{-1}, respectively.

The IR spectra were recorded on a Nicolet IR-470 spectrometer using KBr pellets in the range of 4000–400 cm^{-1}.

3. Results and discussion

3.1. Crystal structure

The crystal structure was found to be a monoclinic system, which belongs to space group C2/c with crystallographic parameters of $a = 2.5282(5)$ nm, $b = 0.59083(12)$ nm, $c = 1.5390(3)$ nm and $\beta = 113.88°$. The volume amounts to $V = 2.1020(7)$ nm^3. With $Z = 4$ molecules per unit cell ($M = 446.62$ for $C_{18}H_{18}N_6S_4$) an X-ray density of $\rho_c = 1.411$ g cm^{-3} was estimated. The bond lengths and bond angles are summarized in Table 1. The ORTEP drawing and the packing diagram are shown in Fig. 1(a) and (b), respectively.

Table 1
Selected bond distances (Å) and angles (°)

Bond distances (Å)		Angles (°)	
S(2)—C(8)	1.736(4)	C(8)—S(2)—C(9)	86.90(17)
S(1)—C(8)	1.742(4)	C(9)—N(2)—N(1)	112.1(2)
N(1)—C(8)	1.384(4)	N(1)—C(8)—S(2)	113.8(3)
N(1)—N(2)	1.311(4)	N(1)—C(8)—S(1)	121.9(3)
N(2)—C(9)	1.350(5)	S(2)—C(8)—S(1)	123.9(2)
N(3)—C(9)	1.350(5)	N(2)—C(9)—N(3)	124.0(3)
Hydrogen bonds			
N3—H1F···N2	3.018	N3—H1F—N2	164.78
N3—H1E···N1	3.038	N3—H1E—N1	164.59

Empirical formula of $C_{18}H_{18}N_6S_2$ suggests that a structure unit includes two molecules, which are connected with each other by intermolecular hydrogen bonds (N2A–H···N3B, N3A–H···N2B) and forms a pair (Fig. 1(a)). Although in one molecule the thiadiazole ring and phenyl ring are not coplanar with the dihedral angle of 34.3°, in one pair the two hydrogen-bonded thiadiazole rings, as well as the N and amino H atoms, which participate the formation of hydrogen bonds, are almost in one plane with mean deviation from plane of 1.4°. The structure units are connected with each other to form a layer also by intermolecular hydrogen bonds, which are formed through the N atoms

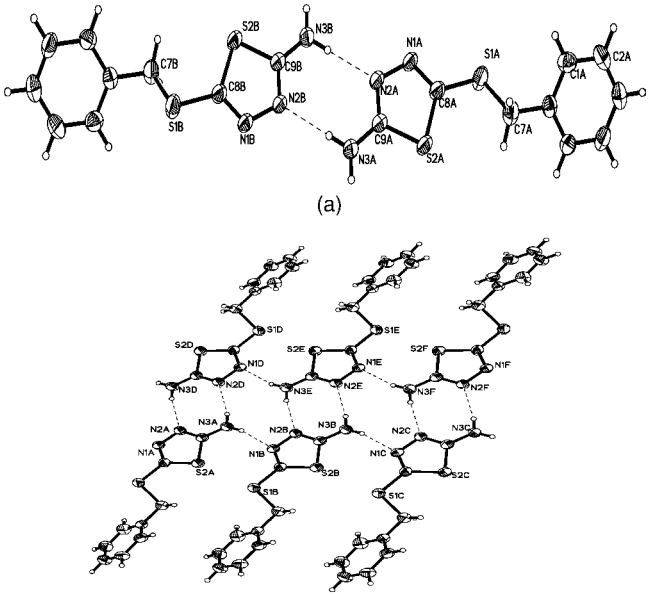

Fig. 1. (a) ORTEP drawing of BSATZ pair; (b) packing diagram of BSATZ layer.

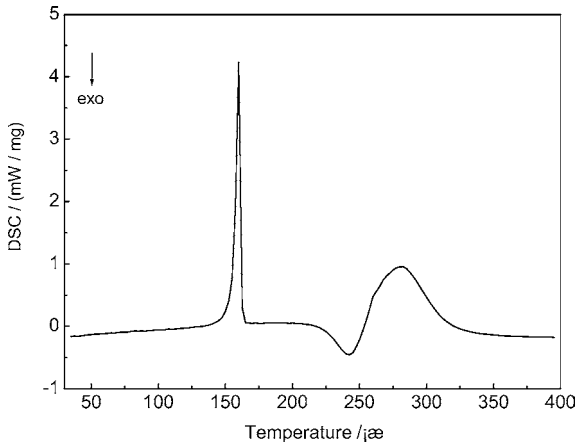

Fig. 2. DSC curve of BSATZ.

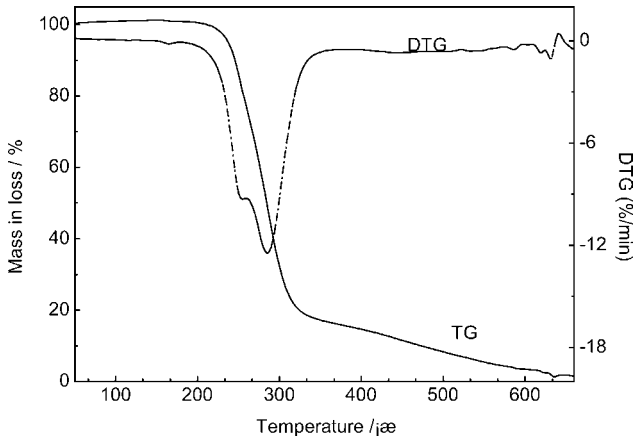

Fig. 3. TG–DTG curve of BSATZ.

(N1) of the thiadiazole rings in one pair and the H atoms of $–NH_2$ group in another pair, i.e. N1–H···N3 (Fig. 1(b)). The existence of phenyl rings at the end of each pair restricts the formation of infinite stretch of the plane and results in the plane extending only in one orientation. As to layer packing, the distance between two planes in neighboring layers is 0.5908 nm, which is bigger than the maximum value for which π–π interactions are accepted [10], as a result, van der Waals force exists between the layers to stabilize the whole structure. This crystal structure is very different from that of a related compound, 2,5-bis-benzylsulfanyl-1,3,4-thiadiazole, in which there are no intermolecular hydrogen bonds formed and only van der Waals force exists. We would report it elsewhere.

3.2. Thermal decomposition of BSATZ

The typical DSC curve of BSATZ is shown in Fig. 2 and TG–DTG curve in Fig. 3. The endothermic peak at 159.6 °C without mass loss, and giving a ΔH value of 119.4 J g^{-1}, is due to the phase change of BSATZ. Thermal decomposition of BSATZ starts at 235.7 °C (on TG curve) and two consecutive transitions can be seen from DTG curve. The first DTG peak appears at 252.5 °C, corresponding to the exothermic peak between 222.6 and 253.4 °C, giving a ΔH value of −52.1 J g^{-1}, and the second peak at 285.3 °C, corresponding to the endothermic peak between 253.4 and 316.1 °C, giving a ΔH value of 235.3 J g^{-1} (on DSC curve). The total mass loss up to 311 °C (on TG curve) is only 77.8%, which is due to the carbon deposition resulted from decomposed products in N_2 atmosphere. The elimination of the carbon is finished at about 660 °C.

The TG curve shows that the two transitions of thermal decomposition process of BSATZ cannot be separated completely. In order to ensure which bond is broken in the first transition of BSATZ, the residues at 255 °C are investigated by IR spectroscopy [11] and the results are listed in Table 2. The absorption peaks at 1507 and 1453 cm^{-1} in IR spectrum of BSATZ, which are assigned to the characteristic vibration band of 1,3,4-thiadiazole rings, exist in the spectrum of the decomposed product, and so do the absorption peaks of benzyl group. Amino group absorption is weakened and only the absorption peak at 1424 cm^{-1}, assigned to C–S vibration, disappeared in the residues. These results justify that the breaking of C–S accompanied by the loss of S element occurs in the first transition of the thermal decomposition.

From the TG and DSC curves it can be seen that the main process of the thermal decomposition of BSATZ occurs in the temperature range of 100–400 °C. In order to simplify the problem only this range would be taken into consideration in the following kinetic analysis.

3.3. Non-isothermal kinetics of BSATZ

3.3.1. Model-free estimation of activation energy

A series of dynamic scans with different heating rates results in a set of data, which exhibits the same degree of conversion (α) at different temperatures. Based on this, two methods are developed by Friedman as well as Ozawa–Flynn–Wall (OFW) to determine the kinetic parameters without having to presuppose a certain model. Fig. 4 shows the TG curves of BSATZ decomposition from 100 to 400 °C with the heating rate of 4.8, 14.7, 219.7 and 29.9 °C min^{-1}, respectively. The

Table 2
IR selected bands (cm^{-1})

Sample	$\upsilon(-NH_2)$	υ()	υ()	υ(S–C)	υ(C–NH_2)	$\upsilon(PhCH_2^-)$
BSATZ	3304, 3106	1517	1507, 1453d	1424	1061	770, 712s
The product at 255 °C	3295w, 3102	1530	1494, 1448d	–	1063w	763, 710s

d, doublet; s, strong; w, weak.

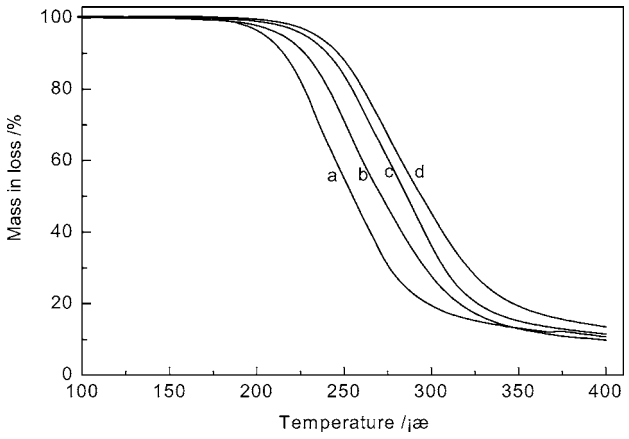

Fig. 4. TG curves of BSATZ with different heating rates (°C min^{-1}): (a) 4.8, (b) 14.7, (c) 19.7, (d) 29.9.

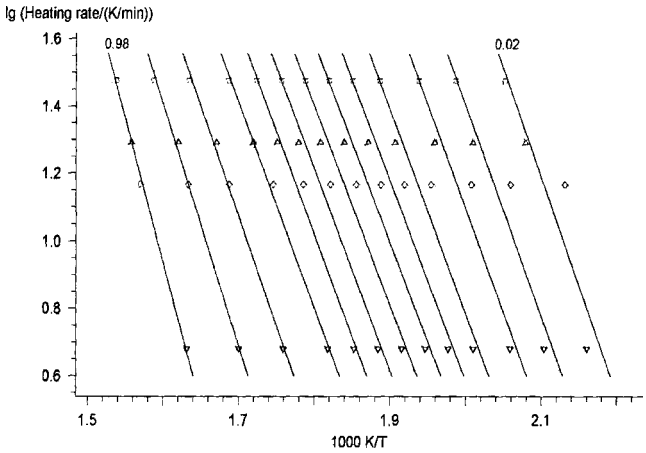

Fig. 5. OFW analysis of BSATZ with β (°C min^{-1}) – ▽: 4.8, ◇: 14.7, △: 19.7, ○: 29.9.

basic data (β, α, T) taken from the TG curves are used in the equations bellow.

Ozawa–Flynn–Wall equation [12,13]

$$\ln \beta = \ln\left(\frac{AE}{R}\right) - \ln g(\alpha) - 5.3305 - 1.052\frac{E}{RT} \quad (1)$$

where β is the heating rate, α the degree of conversion, $g(\alpha)$ the mechanism function, E the activation energy, A the pre-exponential factor, and R the gas constant.

Friedman equation [14]

$$\ln\left(\frac{d\alpha}{dt}\right)_{\alpha=\alpha j} = \ln[A\, f(\alpha)_j] - \frac{E}{RT} \quad (2)$$

where $d\alpha/dt$ is the rate of conversion, and $f(\alpha)$ the mechanism function.

From Eqs. (1) and (2) it is seen that the graphs ln β versus $1/T$ and ln($d\alpha/dt$) versus $1/T$ both show straight lines with slopes $m_{(1)} = -1.052\ E/R$ and $m_{(2)} = -E/R$. The slopes of these straight lines are directly proportional to the reaction activation energy (E). Fig. 5 shows these lines at different α by means of OFW method and the calculated results using both Eqs. (1) and (2) are shown in Table 3.

From Table 3 it can be seen that the values of E and lg A calculated by using different methods are comparable, which indicates that the kinetic parameters thus obtained are reasonable. The dependence of activation energy on the degree of conversion (E_α-dependence) given in Table 3 shows that the activation energy is not a constant and two maximums appear with the extent of decomposition, which indicates that the main process of thermal decomposition of BSATZ is a double-step reaction [15,16].

Kinetic parameters of a reaction can be estimated from the maximums of Friedman method or OFW method, also from the average values of the two methods [17]. According to OFW method, the activation energies and pre-exponential factors of thermal decomposition of BSATZ are, $E_1 = 115.49 \pm 32.58$ kJ mol^{-1}, lg(A_1) (s^{-1}) = 9.19, and $E_2 = 152.62 \pm 6.64$ kJ mol^{-1}, lg(A_2) (s^{-1}) = 11.20, respectively. The values of these parameters would offer initial values for further research into reaction model by means of non-linear regression (NLR) and would be optimized finally.

3.3.2. Multivariate non-linear regression (NLR)

Mode-free method has solved the problem of kinetic parameters and these data can be used to estimate potential

Table 3
Parameters E (kJ mol^{-1}) for the first transitional thermal decomposition of BSATZ

Partial mass loss	Friedman analysis, E (kJ mol^{-1})	lg(A) (s^{-1})	OFW analysis, E (kJ mol^{-1})	lg(A) (s^{-1})
0.02	103.72 ± 21.06	7.87	115.49 ± 32.58	9.19
0.05	106.99 ± 18.53	8.27	111.71 ± 22.31	8.76
0.10	107.00 ± 17.37	8.29	109.82 ± 18.76	8.56
0.20	102.06 ± 15.22	7.80	107.80 ± 16.89	8.36
0.30	100.21 ± 16.67	7.56	105.72 ± 15.81	8.14
0.40	102.81 ± 16.67	7.71	104.29 ± 15.48	7.96
0.50	107.98 ± 12.64	8.10	104.59 ± 14.80	7.94
0.60	112.00 ± 6.92	8.38	106.11 ± 12.27	8.02
0.70	110.52 ± 6.43	8.16	107.63 ± 8.62	8.10
0.80	114.25 ± 8.71	8.35	107.69 ± 4.79	8.01
0.90	129.08 ± 9.24	9.34	115.32 ± 5.49	8.53
0.95	148.77 ± 6.16	10.66	127.95 ± 6.04	9.43
0.98	176.82 ± 22.77	12.61	152.62 ± 6.64	11.20

Table 4
Results of non-linear regression (NLR)

Kinetic parameters	Statistics
lg(A) (s^{-1}): 8.81501	Correlation coefficient: 0.999345
E_1 (kJ mol^{-1}): 111.58851	Rel. precision: 0.001000
React. ord.: 2.16297	Mean of residues: 1.68955
lg(A) (s^{-1}): 7.14611	Max. no. of cycles: 50
E_2 (kJ mol^{-1}): 137.17558	t-critical (0.95; 373): 1.956
FollReact. 1: 1.94276	Durbin–Watson factor: 7.165

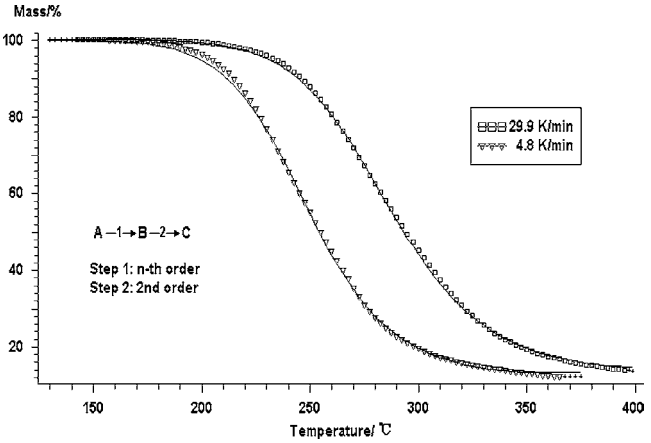

Fig. 6. Fit of TG measurements of BSATZ, simulated with reaction types F_n and F_2 – ▽, □: experimental plots, —: integral plots.

model on which the reaction occurred. Non-linear regression [18] allows a direct fit of the model to the experimental data without a transformation and there are no limitations with respect to the complexity of the model. For this reason, NLR method can be used and iterative procedures can be employed for estimating of the reaction model of BSATZ.

Selecting mechanism function $f(\alpha)$ of different singular reaction types [19]; testing all two-step reaction types to which individual steps are linked as consecutive (d:f), parallel (d:p) and independent (d:i) [19] expect competitive (d:c) model for the fact that the mass loss of the sample is almost independent of heating rates (see Fig. 4) suggests it could not be a competitive model; setting the initial values of the parameters of E and lg A according to Section 3.3.1, the calculation of the regress values is carried out by means of a fifth-degree RUNGE-KUTTA procedure using the Prince-Domand embedding formula for automatic optimization of the number of supporting digits [20]. To minimize the deviance, least squares (LSQ) method is used and a smooth convergence is ensured. All these work are performed under the procedure of NETZCH kinetic software [21].

The calculated curves were obtained by means of NLR. These curves were fitted to the experimental ones and corrected with LSQ. During this procedure in order to get high fitting quality kinetic parameters of initial values are optimized. Considering fitting quality (characterized by correlation coefficient and relative precision), the mechanism of d:f, $A \xrightarrow{F_n} B \xrightarrow{F_2} C$, is the most suitable for this reaction. The kinetic parameters and statistical characterization after the NLR are listed in Table 4 and graphic presentation of the curve fitting are shown in Fig. 6. From Fig. 6 it can be seen that the experimental data and the non-linear regression model fit very well for the fastest and slowest heating rates.

In short, the result of the kinetic analysis above shows that the main reaction of decomposition of BSATZ preferably performs as two-step following reaction: an nth order reaction (F_n) with $n = 2.16$, $E_1 = 111.59$ kJ mol^{-1}, lg(A_1) (s^{-1}) = 8.82, is followed by a second-order reaction (F_2) with $E_2 = 137.16$ kJ mol^{-1}, lg(A_2) (s^{-1}) = 7.15.

Acknowledgements

This work was financially supported by the Natural Science Foundation of China (20271046), the Natural Science Foundation of Henan Province (0211020300) and the Natural Science Foundation of Henan Education Department (20011500027).

References

[1] S.N. Sawhney, A. Gupta, P.K. Sharma, Indian J. Heterocycl. Chem. 1 (1991) 8.
[2] F. Bentiss, M. Lagrene'e, J.P. Wignacourt, Polyhedron 21 (2002) 403.
[3] A.R. Katritzky, A.J. Boulton, Advances in Heterocyclic Chemistry, 9, Academic Press, New York, 1968, pp. 166–170.
[4] Y.J. Gao, Z.S. Wu, Z.J. Zhang, Q.J. Xue, Wear 222 (1998) 129.
[5] A. Gloria, B. Joaquýn, E. Francisco, L.G. Malva, Inorg. Chim. Acta 343 (2003) 60.
[6] F. Clerici, D. Pocar, J. Med. Chem. 44 (2001) 931.
[7] S. Antonaroli, A. Bianco, M. Brufani, L. Cellai, G.L. Baido, et al., J. Med. Chem. 35 (1992) 2697.
[8] J.H. Wang, W. Lei, Y.L. Wang, Chin. J. Syn. Chem. 10 (2002) 314.
[9] G.M. Sheldrick, Acta Crystallogr. Sect. A 46 (1990) 467.
[10] C. Janiak, J. Chem. Soc., Dalton Trans. (2000) 3885.
[11] F. Hipler, R.A. Fischer, J. Müller, J. Chem. Soc., Perkin Trans. 2 (2002) 1620.
[12] T. Ozawa, Bull. Chem. Soc. Jpn. 38 (1965) 1881.
[13] J.H. Flynn, L.H. Wall, Polym. Lett. 4 (1966) 323.
[14] H.L. Friedman, J. Res. Nat. Bur. Stds. 57 (1965) 217.
[15] S. Vyazovkin, Int. Rev. Phys. Chem. 19 (1) (2000) 45.
[16] S. Vyazovkin, Int. J. Chem. Kinet. 28 (1996) 95.
[17] Z.R. Lu, Chin. J. Inorg. Chem. 14 (2) (1998) 119.
[18] P.D.M. Benoit, R.G. Ferillo, A.H. Ganzow, Anal. Chim. Acta 124 (1985) 869.
[19] C.H. Bamford, C.F. Tipper, Comprehensive Chemical Kinetics, vol. 22, Reactions in Solid State, Amsterdam, 1980, pp. 57–63.
[20] G. Netzsch-Geratebau, Thermo-kinetic Analysis Multiple Scan, 3rd ed., pp. 2–44.
[21] G. Netzsch-Geratebau, Thermo-kinetic Software, Version 2000(6a).